2022 IMEKO TC-4 International Conference on
Metrology for Archaeology and Cultural Heritage
University of Calabria, Italy, October 19-21, 2022

Conventional and advanced techniques for archaeological diagnostic of iron artefacts

Martina Bernabale[1], Flavio Cognigni[2], Lorenzo Nigro[3], Marco Rossi[2], Caterina De Vito[1]

[1] Department of Earth Sciences, Sapienza University of Rome, Rome, Italy, martina.bernabale@uniroma1.it
[1]Department of Earth Sciences, Sapienza University of Rome, Rome, Italy, caterina.devito@uniroma1.it
[2]Department of Basic and Applied Sciences for Engineering (SBAI), Sapienza University of Rome, Rome, Italy, flavio.cognigni@uniroma1.it
[2]Department of Basic and Applied Sciences for Engineering (SBAI), Sapienza University of Rome, Rome, Italy; Centro di ricerca e servizi per le Nanotecnologie e le Nanoscienze della Sapienza (CNIS), University of Rome Sapienza, Rome, Italy, marco.rossi@uniroma1.it
[3] Department Italian Institute of Oriental Studies - ISO, Sapienza University of Rome, Circonvallazione Tiburtina 4, Rome, 00185, Italy 3Department, lorenzo.nigro@uniroma1.it

***Abstract* – In this paper, an overview of corrosion processes on iron-based artifacts from Motya (western Sicily, Italy) is proposed. A review of the research contributions is given concerning two main topics: (i) the study of the interaction between iron weapons and the lagoon-like environment of Motya by means of spectroscopic and microscopic analyses. The results are compared with those obtained from the study of armors found in the Punic Necropolis of Lilybaeum (4th century BC, Sicily), which permit to define different corrosion models; (ii) the characterization of corrosion of iron nail (IV century BC) through a multi-modal and multi-scale approach using a X-Ray tomographic technique to get a comprehensive understanding of the structure, morphology, stratification, chemical composition and corrosion mechanisms.**

I. INTRODUCTION

Both the Phoenician sites of Motya (western Sicily, Italy) and the Necropolis of Lilybaeum represent the ideal settings to reconstruct different models of corrosion processes that affected iron artefacts.

In particular, the small Island of Motya is placed in a semi-enclosed coastal marine system, along the western coast of Sicily, between Trapani and Marsala (Figure 1). A peculiar feature of the coastal lagoon is the dynamic equilibrium between freshwater, open sea and wind and wave auxiliary energy inputs. This environment is usually characterized by important physical and chemical gradients, which make it very unstable and prone to unpredictable fluctuations. On the contrary, the Punic Necropolis of Lilybaeum is characterized by burial chambers that are cut into calcarenite rocks, which characterize the sub-soil of Marsala city. In this case, calcarenite rocks protected metal artifacts from fluctuations of temperature and relative humidity, as well as from saline-water infiltration and biological infestations.

As the corrosion process is the result of the interaction between metallic material and environment, it is necessary to accomplish a complete characterization of the corrosion process, combining several analytical techniques that complement each other in information.

The application of a multi-analytical approach performed on cross-sections allowed exploring the patterns of corrosion of artefacts from rim to core.

Fig. 1. Location map of Motya and Lilybaeum in Sicily.

Despite micro-Raman spectroscopy has been extensively used to identify the mineralogical nature of the patina of archaeological objects in a non-invasive way, this technique can be applied on cross-section to characterize the stratigraphy of corrosion layers, because it is capable to finely discriminate between iron corrosion phases occurring at microscopic scale. In fact, it is very important to recognize the location and the connectivity of mineral phases and cracks inside corrosion layer to understand the mechanism of corrosion.

For this reason, in the first case of study a set of weapons and armors found in the 'Archaic Necropolis' of Motya (8^{th}-6^{th} centuries BC, Sicily), along the northern shore of the island, and in the Punic Necropolis of Lilybaeum (4^{th} century BC, Sicily) is investigated through a conventional multi-analytical techniques that includes µ-RS, Scanning Electron Microscopy (SEM-EDS) and Field Emission Scanning Electron Microscopy (HR-FESEM)[1].

Although invasive techniques are usually the only way to explore the deeper spread of corrosion in archaeological iron artifacts from rim to core, the analysis of internal corrosion evolution in the entire object would require excessive sampling and this is not suitable for Cultural Heritage materials.

Therefore, in the second research, in addition to conventional techniques such as SEM-EDS and µ-RS, Multiscale X- ray Microscopy (XRM) has been applied on an iron nail to evaluate if the section, previous analyzed, was representative of the entire sample. The challenge is to extract as much useful information about the spatial distributions of phases in iron-based archeological from 3D visualization and image segmentation[2].

In fact, archaeological iron artefacts undergo corrosion phenomena, resulting in the loss of the metal core, which leads to the loss of information about the function of the object and forging processing.

II. RELATED RESULTS IN THE LITERATURE

In recent years numerous studies dealing with the investigation of corrosion products on iron artifacts have been undertaken. Numerous studies have been addressed on the behavior of archaeological iron artifacts from several environments, such as atmospheric, anoxic, soil, and marine[3,4]. It is well known that corrosion is characterized by stratification in two distinct zones, before reaching the inner metal core, if still present. The first region after the metal core, the so-called dense product layer (DPL), is constituted by iron oxides and oxyhydroxides and appears relatively dense. The second one, *i.e.*, transformed medium (TM), is composed of iron oxyhydroxides and minerals from soil[3].

III. RESULTS AND DISCUSSIONS

A. Rim-core-to-rim analysis

This section reports the summary of the results achieved through the analyses performed on cross-section of weapons and nail.

The Motyan hilt of the sword and the scales armor from Lylibaeum (MM.81.105/2, N.Inv. 4497.2) showed a sandwich structure made up of overlapped layers of corrosion products (Figure 2). The outer layer is composed of a large amount of goethite (α-FeOOH) and soil minerals, (*e.g.*, quartz, calcite, barite, actinolite, microcline), while the inner layer is made of goethite and magnetite (Fe_3O_4). Under alkaline water conditions and moderate salinity, as the lagoon environment of Motya, firstly magnetite is formed by slow oxidation of FeII solution via green rust or Fe $(OH)_2$. After a certain period, the continuous oxidation of iron gives rise to goethite formation, surrounding the initial layer [3,5].

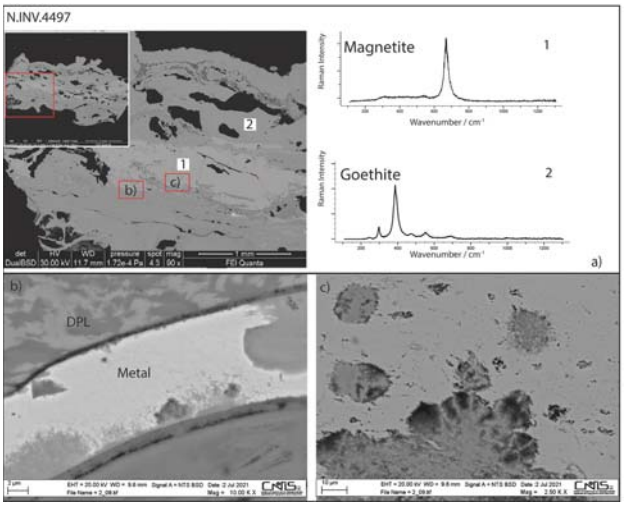

Fig. 2. (a) High-resolution field emission scanning

electron microscopy (SEM-BSE) image showing different areas of sample N. Inv.4497on the left and Raman spectra showing goethite and magnetite on the right. (b) Magnified views marked by red squares show the occurrence of metal surviving, (c) pits of goethite in magnetite matrix

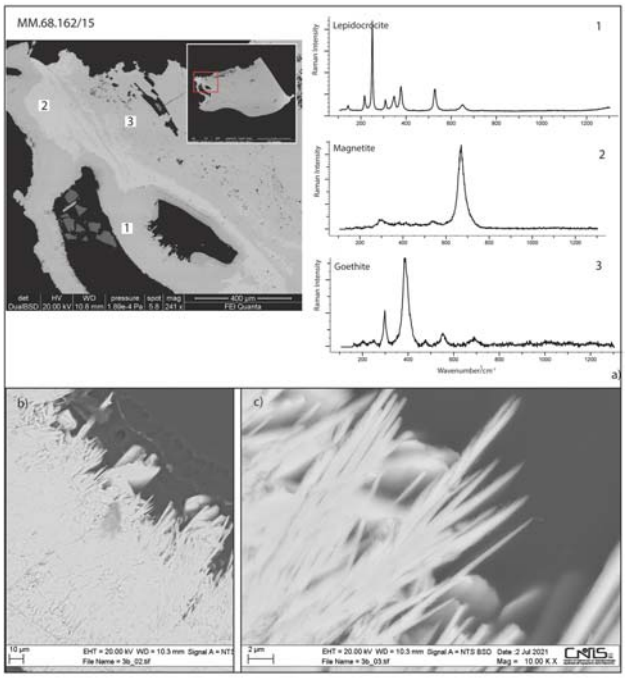

Fig. 3. (a) Scanning electron microscopy-back scattered electron (SEM-BSE) image showing analysis area of sample MM.68.162/15 on the left and Raman spectra of lepidocrocite, goethite, and magnetite on the right. (b,c) High-resolution field emission scanning electron microscopy (HR-FESEM) image showing magnified view of needle-like lepidocrocite

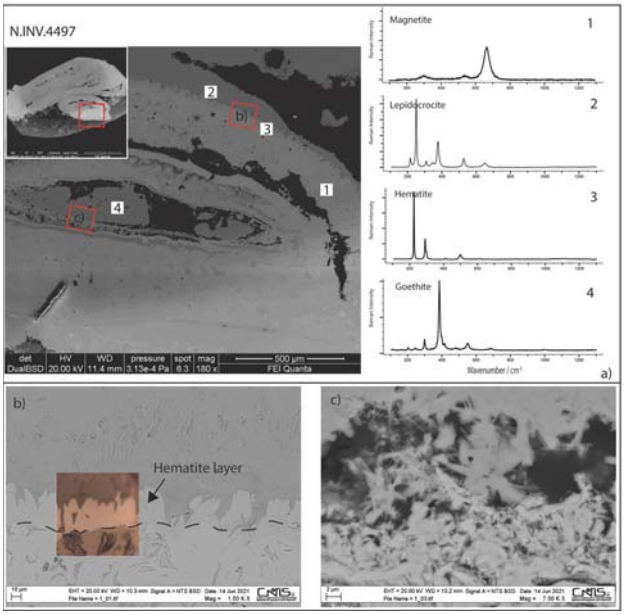

Fig. 4. (a) High-resolution field emission scanning electron microscopy (SEM-BSE) image showing analysis area of sample N. Inv.4497 on the left and Raman spectra showing magnetite, lepidocrocite, hematite, and goethite on the right. (b) High-resolution field emission scanning electron microscopy (HR-FESEM) image showing detail of hematite layer at the forge-welded interfaces and (c) goethite in crack

The spears fragments (MM.78.151/8, MM.78.160/7, MM.68.162/15) from Motya are composed of active corrosion layers made of lepidocrocite (γ-FeOOH) on the top of goethite, which compromised the structure of these artifacts and make the material crumbly and dusty (Figure 3). This type of microstructure matches with the advanced corrosion pattern, that is, thick corrosion layers, described by L'Hostis et al.[5] In these artifacts, a thin layer of magnetite is located on the external part of the sample, whereas goethite is the most abundant phase of the inner part. In this case, the presence of magnetite represents the first stage of corrosion process or the hot forging process of the sample. The direct polymorphic transformation of lepidocrocite into goethite cannot take place in the solid state for both the coordination theory and the different crystal structures. In fact, γ-FeOOH has a cubic close- packed structure of oxygen, whereas α-FeOOH presents a hexagonal close-packed. Therefore, this transformation evolves via dissolution of the γ-FeOOH, followed by the precipitation of intermediate species.

The last type of corrosion identified in the chain mail (N.Inv.4497.1) from Lylibaeum corresponds to a complex and less common type of corrosion consisting mainly of magnetite, covered by a continuous layer of hematite around the ring of the chain mail (Figure 4). The presence of these phases could be explained by a high temperature

corrosion layout, resulting from the hot working of the chain mail during manufacturing. The outer layer is composed of lepidocrocite, which formed by rapid aerial oxidation. The introduction of OH groups into the crystal lattice of magnetite during the conversion in lepidocrocite could be the result of higher activation energy due to high temperature. In addition, the occurrence of crack inside the ring of the chain mail represents another front of access for oxygen and moisture in the artifact. Raman spectra on cross section of chain mail revealed the presence of secondary goethite reprecipitated within the ring of the chain mail. Due to the structural difference between magnetite and goethite, the mechanism of goethite formation inside the ring of the chains can be explained through reconstructive dissolution/ recrystallization reactions.

Chemical, microstructural and mineralogical compositions by SEM-EDS and micro-Raman on cross-section were collected on the tip of the nail (MF.03.53) (Figure 5). The nail shows two corrosion layers: dense product layer (DPL) composed of corroded iron phases and transformed media (TM), where the precipitated iron corrosion phases coexist with some soil elements (Ca, Si, Al) and slag inclusions. From the examination of cross sections, the artefacts seemed to be completely corroded without metal core remaining zones. The DPL shows two substructures, consisting of magnetite and a slightly dark matrix of goethite. The TM layer, instead, is characterized by the presence of goethite and lepidocrocite. First, at the metal/DPL interface, iron oxidizes and generates magnetite. With long-term burial, the corrosion front progresses and forms iron oxyhydroxides (goethite) in which a magnetite strip is present as a presumed trace of the initial layer. Indeed, the main phase observed at the interface between the metal and the rust layer is goethite. The formation of the TM could be explained by the dissolution of iron and reprecipitation of iron corrosion/oxidation products over the surface of the object, perhaps over the original surface.

An interesting aspect is the absence of akageneite and iron chlorides in iron artefacts from Motya. This fact has been confirmed by the low content of Cl detected by chemical analyses. The degree to which Cl^- ions are adsorbed depends on the pH, which increases at low pH (acidic conditions) to balance the excess of H^+ ions on the surface of iron oxyhydroxides. Probably, the alkaline pH conditions characteristic of lagoon-like environment may have favoured the transformation of akageneite into goethite. In fact, the formation of akageneite is a consequence of high Cl^- concentration in acid Fe (II) chloride solutions. On the contrary, lepidocrocite, goethite and magnetite can also form from $FeCl_2$ at lower Cl^- ion levels [6–9].

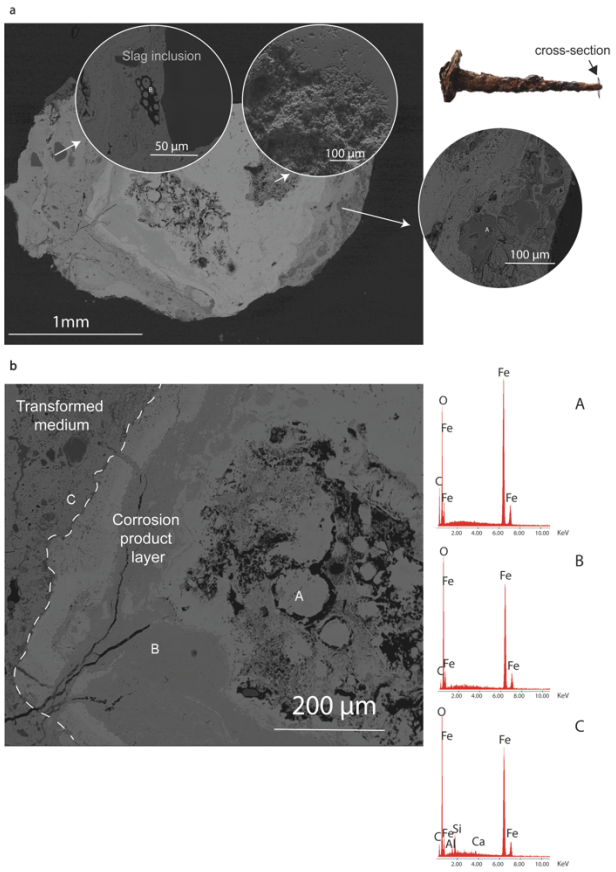

Fig. 5. SEM–EDS images and spectra of the tip of the nail. (a) BSE image of the cross-section with the higher magnification images and spectra of slag inclusion, soil minerals and SE image of the crack. (b) Magnified view of the dense product layer (DPL)

B. Advanced multi-scale analysis

A comprehensive correlative microscopy workflow based on advanced Multiscale X-ray Microscopy (XRM) has been used to characterize corrosion mechanisms in iron-base artifacts to get the maximum information on the whole specimen with the minimum sampling (Figure 6). 2D virtual tomographies of the entire sample allowed us to greatly increase the performance of the traditional analyses with a minimal sampling processing (Figure 7). In addition, the potential of XRM is employed to explore the corrosion propagation and verify the presence and the thickness of metal core in the entire object, monitoring the variations in density between different phases of the artefact. Indeed, sub-micron X-ray microscope ZEISS Xradia Versa 610 overcomes the limits of X-ray computed tomography (CT), offering a setup that enables non-destructive, multi-length scale visualization with an imaging field of view range from tens of millimeters down to tens of micrometers, and a true spatial resolution of 500 nm.

XRM reveals the existence of an internal metal core, starting from a few millimeters above the tip of the nail and showing that the tip is completely corroded away. In contrast, the head and upper part of the shank are well preserved. Nail 3D reconstruction and segmentation allow evaluating quantitatively the presence of each phase of the nail in virtual slices. However, the low-resolution scan represents a limiting factor for the identification of the corrosion sub-layers. Thus, to tackle the complete characterization of the virtual section which includes the metal remaining, high-resolution scan is also performed, covering all length scales from micrometric resolution to centimeters (Figure 8).

These insights are fundamental to characterize the manufacturing and performing features of an artefact and reach an extended knowledge of ancient population technological background.

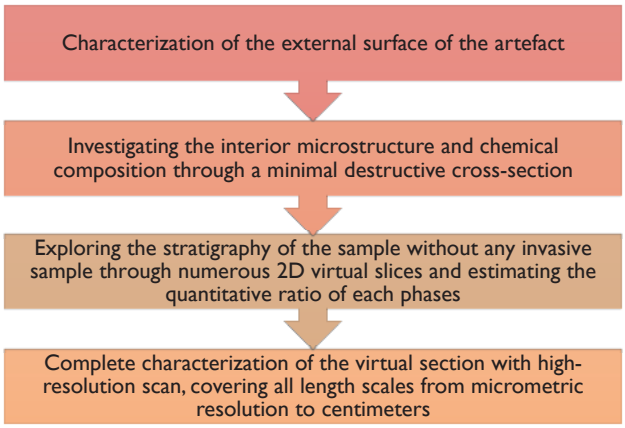

Fig. 6. The comprehensive workflow

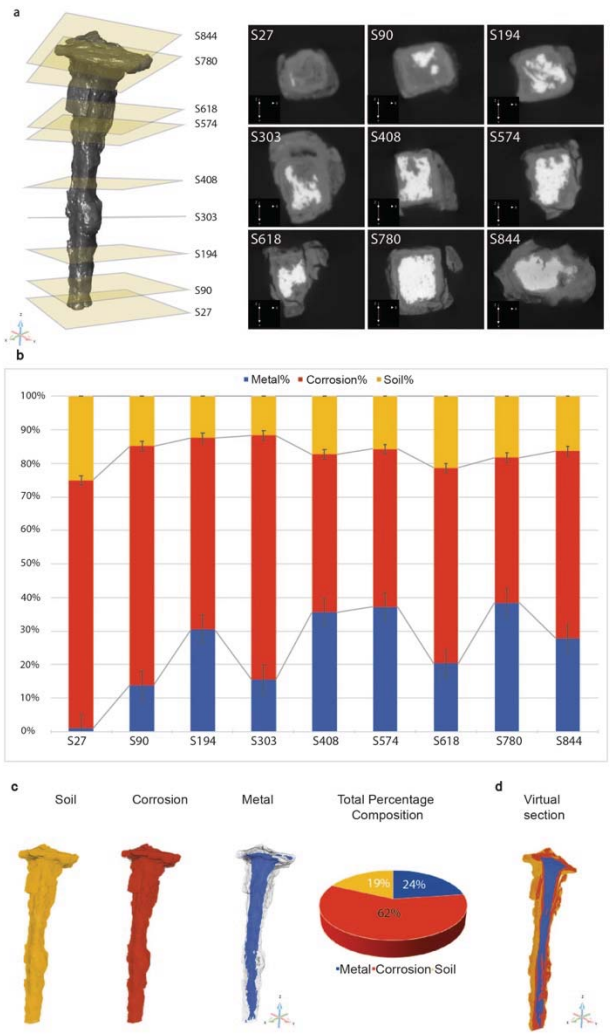

Fig. 7. Low-resolution scans and 3D reconstruction of the nail. (a) On the left, the exact position of each virtual cross section in the nail shown on the right. (b) Histogram quantifying percentages of metal, corrosion and soil per each slice shown in a. (c) 3D reconstruction of the nail and segmentation of different layers: yellow—soil, red—corrosion layer, blue—metal; on the right, pie chart indicating the total percentages composition resulted by imaging segmentation. (d) Sagittal section of the 3D reconstruction showing the internal region of one half of the nail.

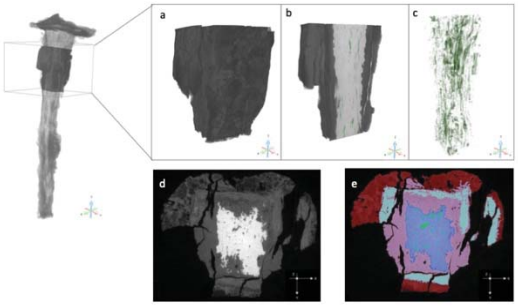

Fig. 8. High-resolution scans of a selected volume of the nails. (a) 3D rendering of analysed section (b) Sagittal cut of the 3D reconstruction, showing parallel structural discontinuities (c) 3D segmentation of structural discontinuities (green) (d) 2D slice, showing microstructure detail and corrosion stratigraphy in grayscale value (e) Segmented 2D slice in false colors: metal in blue, DPL in pink (goethite) and turquoise (magnetite) and TM (red).

IV. CONCLUSION

An evolutionary two-steps approach for the study of corrosion in iron artefacts is presented.

In the first step, traditional techniques are applied to reconstruct different corrosion models, highlighting the polymorphic inter-conversions and dissolution-re-precipitation reactions that occurred among iron oxy-hydroxides in the archaeological sites of Motya and Lilybaeum. Indeed, although the opposite procedure is more intuitive, chemical, microstructural and mineralogical information carried out with invasive techniques on a small portion of the artefact are the necessary starting point for more sophisticated non-invasive analyzes, such as XRM, which does not allow obtaining chemical information on the material. In fact, routine analyzes can give precise indications on the type of material, on the manufacturing techniques and on the state of deterioration, suggesting the type of diagnostic work to be developed.

In the second step, XRM workflow resulted to be an appropriate technique for monitoring the corrosion stratigraphy of an iron nail that revealed the presence of uncorroded nucleus inside the head and in the upper part of shank of an archaeological nail.

Future work will be devoted to applying this workflow to the identification of corrosion propagation in more complex artefacts.

V. ACKNOWLEDGMENTS

This work has been partially funded by ATOM project (Advanced TOmography and Microscopies) granted by Regione Lazio with the call “Open Infrastructure for research” (G11949, 04.09.2017) 2017. The authors thank Dr. Francesco Mura for FESEM imaging and analyses.

REFERENCES

[1] M. Bernabale, L. Nigro, C. Vaccaro, M. Nicoli, D. Montanari, P. Bigini, C. De Vito, Micro-Raman spectroscopy and complementary techniques for the study of iron weapons from Motya and Lilybaeum (Sicily, Italy): Corrosion patterns in lagoon-like and calcarenitic hypogea environments, J. Raman Spectrosc. (2022) 272–287. doi:10.1002/jrs.6285.

[2] M. Bernabale, F. Cognigni, L. Nigro, M. Rossi, T. De Caro, C. De Vito, A comprehensive strategy for exploring corrosion in iron - based artefacts through advanced Multiscale X - ray Microscopy, Sci. Rep. (2022) 1–9. doi:10.1038/s41598-022-10151-w.

[3] D. Neff, P. Dillmann, L. Bellot-Gurlet, G. Beranger, Corrosion of iron archaeological artefacts in soil: Characterisation of the corrosion system, Corros. Sci. 47 (2005) 515–535. doi:10.1016/j.corsci.2004.05.029.

[4] E. Estalayo, J. Aramendia, J. M. Matés Luque, J. M. Madariaga, Chemical study of degradation processes in ancient metallic materials rescued from underwater medium. J. Raman Spectrosc. 50(2) (2019) 289-298.

[5] V. L’Hostis, D. Neff, L. Bellot-Gurlet, P. Dillmann, Characterization of long-term corrosion of rebars embedded in concretes sampled on French historical buildings aged from 50 to 80 years, Mater. Corros. 60 (2009) 93–98. doi:10.1002/maco.200805019.

[6] B. Jegdić, S. Polić-Radovanović, S. Ristić, A. Alil, Corrosion processes, nature and composition of corrosion products on iron artefacts of weaponry, Sci. Tech. Rev. 61 (2011) 50–56.

[7] L.S. Selwyn, P.I. Sirois, V. Argyropoulos, The corrosion of excavated archaeological iron with details on weeping and akaganeite, Stud. Conserv. 44 (1999) 217–232.

[8] P. Refait, J.M.R. Génin, The mechanisms of oxidation of ferrous hydroxychloride β-Fe2(OH)3Cl in aqueous solution: The formation of akaganeite vs goethite, Corros. Sci. 39 (1997) 539–553. doi:10.1016/S0010-938X(97)86102-1.

[9] Q. Wang, An investigation of deterioration of archaeological iron, Stud. Conserv. 52 (2007) 125–134. doi:10.1179/sic.2007.52.2.125.